First Description of a Multisystemic and Lethal SARS-CoV-2 Variant of Concern P.1 (Gamma) Infection in a FeLV-Positive Cat: New Concerns Regarding Viral Re-emergence and Adaption to Pets

Rodrigo Lima Carneiro
Bahia State University
Jessica Pires Farias
Federal University of Western Bahia
Josilene Ramos Pinheiro
Federal University of Western Bahia
Jackson Farias
Bahia State University
Andre Carloto Vielmo
Federal University of Western Bahia
Alexander Birbrair
Universidade Federal de Minas Gerais
Aline Belmok
University of Brasília
Fernando Lucas Melo
University of Brasília
Bergmann Moraes Ribeiro
University of Brasília
Gepoliano Chaves
University of Chicago
Paloma Oliveira Vidal
Federal University of Western Bahia
Wilson Barros Luiz
State University of Santa Cruz
Jaime Henrique Amorim (jaime.amorim@ufob.edu.br)
Federal University of Western Bahia

Research Article

Keywords: COVID-19, cats, SARS-CoV-2, transmission, multi-systemic viral infection

Posted Date: November 22nd, 2021

DOI: https://doi.org/10.21203/rs.3.rs-1074163/v1

Abstract

Background: Coronaviruses are recognized for their ability to

cross the species barrier and infect new hosts. The coronavirus disease 2019 (COVID-19) is caused by the new coronavirus SARS-CoV-2 (*Severe acute respiratory syndrome coronavirus 2*). It remains unclear whether other animals, including pets, are crucial in the spread and maintenance of COVID-19 worldwide.

Methods: In this study, we analysed the first fatal case of a SARS-CoV-2 and FeLV (*Feline leukemia virus*) co-infection of an eight-year-old male cat. We carried out a clinical evaluation, pathological analysis, and viral genomic analysis.

Results: As main results, we observed an animal presenting severe acute respiratory syndrome and lesions in several organs, which led to animal's death. The causative agent was confirmed to be SARS-CoV-2, variant of concern P.1 (Gamma). The virus presented a pattern of mutations potentially associated with feline infection. In addition, the virus was detected by RT-qPCR in the spleen, liver, heart, lungs, trachea, intestines and kidneys, indicating a multisystemic viral infection. The virus was found in a high load in the trachea, suggesting a capacity of transmitting the virus.

Conclusion: Our data show that felines, such as FeLV-positive cats, are susceptible to SARS-CoV-2 infection, and may be intermediate hosts in this pandemic.

Introduction

Viruses from the *Coronaviridae* family are recognized for their ability to
cross the species barrier and establish new host reservoirs of infection [1]. A disease (COVID-19, coronavirus disease 2019) caused by a new coronavirus (SARS-CoV-2, *Severe acute respiratory syndrome coronavirus 2*) emerged in 2019 and was declared as a pandemic on March 11, 2020. According to the World Health Organization, more than 250 million of cases and more than 5 million of deaths were attributed to COVID-19 since its initial report in late 2019 [2].

Phylogenetic studies indicate bats as original hosts of SARS-CoV-2. However, the species barrier jump from bats to humans is considered unlikely. The most probable hypothesis includes the existence of an intermediate host [3]. Such a scenario points out the importance of animals in the spread and even maintenance of COVID-19 worldwide. Such a maintenance could be supported by events of reverse zoonosis, which was previously reported for dogs, cats, farmed minks and zoo big felines [4,5]. This may represent a threat for the health of pets, zoo and wild animals. In addition, the replication of SARS-CoV-2 in animals represents a constant risk of emergence of new variants with potential to threat human health and to challenge the protective efficacy of vaccines currently available. This further emphasizes the need of a One Health approach to tackle SARS-CoV-2 re-emergence.

In this study we show clinical and laboratory aspects of a fatal case of SARS-CoV-2 and FeLV (*Feline leukemia virus*) co-infection of a male cat. Detailed data presented here will be useful to recognize and better manage animals which are more susceptible to SARS-CoV-2 infection. Results presented here will be useful in efforts to avoid re-emergence of this coronavirus mediated by pets.

Methods

Ethics and animal experimentation

All handling procedures and experiments involving the animal were approved by the Committee for the Ethical Use of Animals in Research of the State Bahia University (nº 2021.005.0018150-89). All procedures involving the animal were carried out in accordance with the ethical and biosafety guidelines.

Clinical evaluation

An eight-year-old male domestic cat of undefined breed was admitted with respiratory syndrome at a veterinary clinic in Barreiras city, Bahia, Brazil. Data regarding respiratory aspects, temperature, heartbeat, weight, and other clinical aspects were kept during anamnesis. Laboratory analyses were required due to the clinical condition of the animal.

Bloods cell counts, biochemical and serological analysis

Complete blood cell counts (CBC) were performed using fresh blood samples with ethylenediaminetetraacetic acid (EDTA) at 2% (w/v). Analyses were carried out using an automated Hematoclin 2.8 VET instrument (Bioclin, Brazil), according to manufacturer
$s \in structions. Inaddition, serum \leq velsofglucose, urea, creat \in \in e, alan \in e$ and a min $otranerase, alkal \in ephospâse,$ and $\gamma glutamyltra$
s instructions. Serological tests for *Feline immunodeficiency virus* (FIV) and *Feline leukemia virus* (FeLV) were carried out using the FIV AC / FeLV AG COMBO VET FAST VET 013-1 (BIOCLIN, Brazil). Moreover, a serological analysis for *Feline infectious peritonitis virus* (FIPV) was carried out using an ImmunoComb antibody test kit (VP DIAGNOSTICO, Brazil). Those Dot ELISA analysis were carried out according to the manufacturer's recommended protocols.

Imaging Diagnostics

Thoracic radiography procedure was performed using a digital imaging equipment
(ECORAY, Korea) with 70 kV of potency and 1.2 milliampere seconds (mAs) as the radiographic technique. To evaluate respiratory conditions, right and left lateral and ventrodorsal projections were chosen. The entire procedure lasted 2 minutes.

Necropsy and samples collection

The *postmortem* examination was performed immediately after the death, and the macroscopic changes were recorded using a digital camera. At necropsy, the body was placed in the supine position for a superficial mento-pubic incision. To improve the exposure of pelvis and thorax, the hind limbs were disarticulated at the level of the hip joint and the forelegs folded down laterally dissecting the skin and subcutaneous tissue of the submandibular and cervical regions. Afterwards, costochondral disarticulation was performed in all fixation points of the ribs and the cranial and caudal pubic branches were incised. After hyoid disarticulation, the trachea and esophagus were released between the cervical muscle fascia and the entrance to the thoracic cavity, and the monobloc was pulled so that it could be detached along the entire thoracic extension to the diaphragm. Then, the diaphragm was sectioned in the dorsal semicircular portion, making a small incision in the right kidney, and continuously sectioning the abdominal set parallel to the vertebral column up to the pelvic cavity. Finally, the pelvic cavity was contoured along with the external genitalia and anus so that the monobloc was released entirely from the cadaver.

Tissue samples of kidneys, lungs, heart, trachea, liver, intestines, and spleen were stored in 10% formaldehyde at room temperature or as fresh tissues at −80°C until analysis.

Gross pathology and histopathology

Macroscopic evaluation of organs considered characteristics such as edema, congestion, discoloration, atelectasis, and consolidation. Tissues samples from kidneys, lungs, heart, trachea, liver, intestines, and spleen with standardized size of 2.0 x 1.6 x 1.2 cm were fixed overnight in a 4% formaldehyde solution and buffered with sodium phosphate 0.1 M at pH 7.2. After dehydration with ethanol, the fragments were placed in xylol and then paraffined. The samples were blocked using a TP 1020® sample blocker (LEICA, Germany) and microtomized using a RM 2255 rotary microtome (LEICA, Germany), according to manufacturer`s instructions. After that, the samples were stained with hematoxylin and eosin.

RNA extraction and reverse transcription quantitative PCR (RT-qPCR)

Nucleic acid extraction was carried out from tissue samples of the seven organs of the feline: lungs, trachea, spleen, liver, intestines, heart and kidneys. Samples were prepared by adding 1 mL of Quik-Zol Trizol reagent (LUDWIG BIOTECNOLOGIA, Brazil) for each 100 mg of tissue and homogenized by vortexing. After this process, 250 µL of each sample was loaded onto columns of Cellco-Virus RNA + DNA Preparation Kit Spin (CELLCO BIOTEC, Brazil), and RNA was purified according to manufacturer`s instructions.

The detection of SARS-CoV-2 was performed using the Allplex™ 2019-nCov Assay (SEEGENE, South Korea), according to manufacturer`s instructions. Thermocycling was carried out in a QuantStudio 5 instrument (Applied Biosystems, USA) with a hold stage composed of a first step of 20 min at 50°C, followed by a second step of 15 s at 95 °C. The PCR stage was composed of a first step of 15 s at 94°C followed by a second step of 30 s at 58 °C, repeated 45 times.

SARS-CoV-2 Genome Sequencing

The RNA extracted from the seven feline samples were submitted to Next Generation Sequence. RNA extractions (8 µL) from tissue samples were submitted to reverse transcription with LunaScript® (NEB, USA), following manufacturer`s instructions. The obtained cDNA was used as template for SARS-CoV-2 genome amplification with 1200bp amplicon "midnight" primer set V5, as previously described (https://www.protocols.io/view/sars-cov2-genome-sequencing-protocol-1200bp-amplic-btsrnnd6?step=4). Two tiling-based PCR were performed using Q5 Hot Start High-Fidelity DNA Polymerase (NEB, USA) and primers as previously described (https://www.protocols.io/view/sars-cov2-genome-sequencing-protocol-1200bp-amplic-btsrnnd6?step=4). Termocycling was composed of an incubation for 30 s at 98 °C for denaturation, followed by 35 cycles of 98 °C for 15 s and 65 °C for 5 min for annealing and extension. PCR amplicons for pool 1 and pool 2 were combined for each sample and adjusted to a concentration of 5 -10 ng/µL. End-Prep reactions were performed with NEBNext® Ultra™ II End Repair/dA-Tailing Module (NEB, USA) and barcoded using ONT Native Barcoding Expansion kit (EXP-NBD104) (Oxford Nanopore Technologies, UK), according to manufacturers`s protocols. The barcoded samples were then combined and purified using AMPure XP Beads (Beckman Coulter, USA) and loaded onto Oxford Nanopore MinION SpotON Flow Cells R9.4.1 (Oxford Nanopore Technologies, UK). High accuracy base calling was carried out after sequencing from the fast5 files using the Oxford Nanopore Guppy tool (Oxford Nanopore Technologies, UK).

Mapping, primer trimming, variant calling and consensus assembly building were performed with artic-ncov2019 pipeline, using the Medaka protocol (https://artic.network/ncov-2019). The genome was assembled with at least 20x coverage. Pango lineage was attributed to the newly assembled genome using the Pangolin v3.1.11 software tool (https://pangolin.cog-uk.io/).

Study of viral genetic polymorphisms

Mutations were detected using FASTA sequences downloaded from GISAID on October 09, 2021. SARS-CoV-2 variants were called using a customized script written in bash. Bash script processing of FASTA samples produced a Variant Call Format file (VCF) for each sample. VCF files were then merged using bcftools. In the merged VCF file, we identified 813 mutations present in FASTA sequences isolated from felines (See Supplementary data-sheets 1 and 2). In order to study the potential existence of mutations characteristic of SARS-CoV-2 that infected deceased animals only, unsupervised hierarchical clustering analysis was performed using R version 4.1.0 and R library pheatmap version 1.0.12. 813 mutations identified in viral sequences isolated from animals were used to classify groups of FASTA samples using the mutation frequency of each group of interest. The groups of interest represented sequences from these 10 different origins: FASTA sequences from the Brazilian bordering states of Bahia, Tocantins and Goias; FASTA sequences from Brazil between January-February 2021 and Brazil between March-April 2021; FASTA sequences from Deceased, Alive and Unknown Deceased status animals; FASTA sequences from Manis javanica and Manis polydactila and FASTA sequences from bats of the genus Rhinolophus. All sequences were downloaded from GISAID. Frequencies of the 813 mutations detected in viruses that infected cats were then used to classify these groups using the unsupervised hierarchical clustering method. 68/813 (8.35%) mutations allowed unsupervised classification of the sequences of deceased animals and their separation from non-deceased animals.

Results

Clinical evaluation and diagnosis of severe acute respiratory syndrome

An eight-year-old male domestic cat of undefined breedwas admitted at a veterinary clinic in Barreiras city, Bahia, Brazil, presenting intense dyspnea, cyanotic mucous and whisper in right hemitorax auscult. The animal was previously exposed to its owner, who was confirmed to be infected by SARS-CoV-2 (data not shown). Pet`s body temperature was considered as normal for cats (38.6 °C). The oxygen saturation was shown to be of 87%. In addition, thoracic radiography showed increased radiopacity in the cranial and caudal lobes of lungs, as well as peribronchial infiltrates compatible with incipient bronchitis, as evidenciated by radiographic views of ventrodorsal (Fig. 1A) and right (Fig. 1B) and left (Fig. 1C) sides, indicating an acute pneumonia. The animal presented severe respiratory failure four hours later and died. Altogether, these results indicate that the cat suffered a severe acute respiratory syndrome. Blood samples were collected before the death aiming haematological, serological and biochemical analyses.

Hematological, serological and biochemical analyses

Regarding haematological findings, we found lymphocytopenia (2,2 lymphocytes/mm^3 in WBC), anemia (RBC=1, 41 x 10^{12} erytrocytes/L; Haemoglobin = 3,0 g/dL) and severe thrombocytopenia (17 x 10^9 platelets/L). Regarding serum biochemical markers increased levels of urea (71.20 mg/dL) and glucose (176 mg/dL) were found. Furthermore, the diagnosis of FIV/FeLV infections performed by serological tests showed a positive result for FeLV, which has been associated with immunosuppression and all of the haematological disturbances observed.

Detection of viral RNA and genome sequencing

Viral RNA was detected in all collected fresh tissues (see Table 1). According to cycle threshold (CT) values, the highest viral load was found in trachea, followed by those of liver, spleen, heart, lungs, kidneys and intestines. The presence of viral RNA in all of these tissue samples indicate a multisystemic viral infection. In addition, the virus was confirmed to be a variant of concern P.1 (Gamma), as shown by genome sequencing. The sequence was deposited at GISAID (EPI_ISL_4565991).

Study of viral genetic polymorphisms

As shown in Figure 6 and Supplementary Figures 1 and 2, viral sequences of non-human sources (Manis and Rhinilophus) were compared to sequences of feline source and sequences of human source from Brazil and the three neighboring States of Bahia, Tocantins and Goias. In this analysis, mutation frequencies allowed Manis and Rhinolophus to organize into a single cluster. In the next cluster, mutation frequencies of all regions of Brazil were grouped together while in the same cluster, feline sequences of deceased animals were classified separated from sequences of living animals and sequences from animals of unknown deceased status. Together these results suggest the identification of mutations potentially associated with feline survival status. The little availability of sequences known to be associated with pet decease requires further investigation of the association identified here.

Postmorten evaluation

Collapsed and emphysematous areas with air distending the interlobular septa of the lungs were seen in gross pathology (Fig. 2A and 2B). In addition, the kidneys were shown to be pallid, shorter, irregular and firm. With a cross-section, the cortical region had a reduced thickness and there was a secretion with a catarrhal aspect in the calyxes and pelvis (Figure 2C). Collectively, these results indicate severe damages in lungs and kidneys of the feline that was co-infected by SARS-CoV-2 and FeLV.

Histopathology

Histopathological investigation showed specific microscopic changes in trachea, lungs, liver and kidneys. Histological sections of the trachea and kidneys reveled multifocal lymphoplasmacytic inflammatory infiltrate, which indicates tracheitis (Fig. 3 A-D) and moderate lymphoplasmacytic interstitial nephritis (Fig. 3 E-H), respectively (Figure 3). The lung sections, in turn, revealed multiple areas of atelectasis (Fig. 4A). In addition, compensatory emphysema foci (Fig. 4B) and a sparse inflammatory infiltrate associated with the peri bronchial mucous glands were observed (Figure 4 A-G). Furthermore, liver microscopy revealed vacuolar degeneration of hepatocytes, seen in periportal hepatitis. Hepatic lymphoplasmacytic infiltrations were mild (Figure 5). Collectively, these histopathologic results reinforce that trachea, lungs, liver and kidneys were severely damaged by SARS-CoV-2 infection.

Discussion

SARS-CoV-2 most probably crossed the species barriers and established humans as new host reservoirs of infection using first an intermediate host [6]. It is possible that animals, including pets, have an unrevealed importance in the spread and even maintenance of COVID-19 worldwide. Events of reverse zoonosis could support such a maintenance. The replication of SARS-CoV-2 in animals represents a constant risk of emergence of new variants with potential to threat human health and to challenge the protective efficacy of vaccines currently available [7]. In addition, it is important to highlight that animals are not being vaccinated against COVID-19.

In this study, we presented the first evidence of a multisystemic and lethal SARS-CoV-2 infection in cat. The multysystemic distribution of the virus was confirmed by its detection in several organs, including kidneys and intestines. These findings point to the risk of environmental contamination by urine or feces. In addition, the high viral load seen in trachea points to the risk of transmission of SARS-CoV-2 to other animals or even humans. Moreover, this is the first report of an animal case infected by the SARS-CoV-2 variant of concern (VOC) P.1 (Gamma) worldwide. Such a VOC caused a dramatic health crisis in Brazil and other countries of South America [8–10] due to its high infectivity and immune escape capacity [11]. We highlight that during the time of the cat`s infection, a large number of infections caused by VOC P.1 was registered in Bahia, which moved the state health department to suspend non-essential trips

[12]. This scenario may have increased the chance of pet infections. In addition, our results show that there are SASR-CoV-2 mutations potentially associated with feline infection. Such mutations are distributed in viruses of different lineages. It is an important evidence that there are SARS-CoV-2 variants adapted to pets.

It is also important to highlight that the cat was FeLV-positive. Such a co-infection may have increased the severity of the COVID-19 seen in that animal, which involved a very clear severe acute respiratory syndrome. The FeLV [11] is a retrovirus that infects cats. Contaminated saliva or nasal secretions transmit the virus, which is capable of compromising the animal`s immune system [12]. In this study, we observed haematological disturbances that are related to FeLV infection. In general, such pathological signs are accompanied by immunosuppression [13]. We hypothesize that beyond the FeLV/SARS-CoV-2 co-infection led to a lethal severe acute respiratory syndrome it also enhanced the viral load in organs that can contribute to both, environmental contamination and direct transmission of the coronavirus. In addition, such a co-infection may represent a threat for FeLV-positive cats and should be carefully investigated in cases of clinical suspects. In this context, detailed pathologic data presented here should be used to better recognize and manage cats that are more susceptible to SARS-CoV-2 infection.

Conclusion

Our study indicates that replication of SARS-CoV-2 in high loads is fully possible in FeLV-positive cats. In addition, we found mutations potentially associated with infection of felines. This represents a constant risk of emergence of new variants with potential to threat human health and to challenge the protective efficacy of vaccines. Pets should be surveilled with regard to SARS-CoV-2 infection. The need for a strong and engaged One Health approach in all areas of the world is essential to tackle SARS-CoV-2 re-emergence.

Abbreviations

COVID-19: coronavirus disease 2019; SARS-CoV-2: *Severe acute respiratory syndrome coronavirus 2;* FeLV: *Feline leukemia virus;* CBC: Complete blood cell counts; EDTA: ethylenediaminetetraacetic acid: PCR: polymerase chain reaction; RNA: ribonucleic acid; cDNA: complementary deoxyribonucleic acid; GISAID: global initiative on sharing avian influenza data; WBC: white blood cells; RBC: red blood cells; FIV: *Feline immunodeficiency virus*; VOC: variant of concern.

Declarations

Acknowledgements

We are thankful to Consórcio Multifinalitário do Oeste da Bahia and 27968 FINEP/RTR/PRPq/REDE COVID-19 for providing financial support to Jaime Henrique Amorim. We are also thankful to Instituto Serrapilheira/Serra-1708-15285 for providing financial support to Alexander Birbrair. Furthermore, we appreciate the contribution of CLIMEV veterinary clinic to the animal care and handling.

Author's contributions

RLC and JPF conceived the study, carried out clinical and molecular analyses and interpreted the data generated; JF and ACV performed hematological, biochemistry, serological and image analysis; JRP, AB, POV, GC, FLM and BMR performed the genome sequencing experiments and analysis; WBL; AB and JHA supervised the study and interpreted the data generated. JPF, AB and JHA wrote the manuscript.

Funding

Jaime Henrique Amorim is supported by grants from Consórcio Multifinalitário do Oeste da Bahia and 27968 FINEP/RTR/PRPq/REDE COVID-19. Alexander Birbrair is supported by a grant from Instituto Serrapilheira/Serra-1708-15285. This work was partially supported by Coordenação de Aperfeiçoamento de Pessoal de Nível Superior (CAPES) (Edital nº 9/2020 Prevenção e Combate a Surtos, Endemias, Epidemias e Pandemias" Project number: 88887.504570/2020-00); Rede Corona-ômica BR MCTI/FINEP (Financiadora de Estudos e Projetos, FINEP Project number: 01.20.0029.000462/20)

Availability of data and materials

Genomic data was deposited to GISAID. Other data will be provided under request.

Ethical approval and consent to participate

All handling procedures and experiments involving the animal were approved by the Committee for the Ethical Use of Animals in Research of the State Bahia University (nº 2021.005.0018150-89).

Consent for publication

All the authors of this manuscript agreed to publish this research work.

Competing interests

All authors declare that they have no competing interests.

References

1. RL G, RS B. Recombination, reservoirs, and the modular spike: mechanisms of coronavirus cross-species transmission. J Virol [Internet]. J Virol; 2010 [cited 2021 Aug 17];84:3134–46. Available from: https://pubmed.ncbi.nlm.nih.gov/19906932/

2. WHO Coronavirus (COVID-19) Dashboard | WHO Coronavirus Disease (COVID-19) Dashboard.

3. Andersen KG, Rambaut A, Lipkin WI, Holmes EC, Garry RF. The proximal origin of SARS-CoV-2. Nat Med. 2020;2–4.

4. THC S, CJ B, SM I, KWS T, PYT L, EMW T, et al. Infection of dogs with SARS-CoV-2. Nature [Internet]. Nature; 2020 [cited 2021 Aug 17];586:776–8. Available from: https://pubmed.ncbi.nlm.nih.gov/32408337/

5. N O, RJ M, S V, F H, BB OM, RW H der H, et al. SARS-CoV-2 infection in farmed minks, the Netherlands, April and May 2020. Euro Surveill [Internet]. Euro Surveill; 2020 [cited 2021 Aug 17];25. Available from: https://pubmed.ncbi.nlm.nih.gov/32553059/

6. Segalés J, Puig M, Rodon J, Avila-nieto C, Carrillo J, Cantero G. Detection of SARS-CoV-2 in a cat owned by a COVID-19 – affected patient in Spain. 2020;117:24790–3.

7. He S, Han J, Lichtfouse E. Backward transmission of COVID-19 from humans to animals may propagate reinfections and induce vaccine failure. Environ. Chem. Lett. Springer Science and Business Media Deutschland GmbH; 2021. p. 763–8.

8. Taylor L. Covid-19: How the Brazil variant took hold of South America. BMJ. BMJ Publishing Group; 2021;373.

9. Taylor L. Covid-19: Brazil breaks record daily death toll as crisis spreads through South America. BMJ. NLM (Medline); 2021;373:n930.

10. Taylor L. Covid-19: Brazil's spiralling crisis is increasingly affecting young people. BMJ [Internet]. British Medical Journal Publishing Group; 2021 [cited 2021 Oct 5];373:n879. Available from: https://www.bmj.com/content/373/bmj.n879

11. Naveca FG, Nascimento V, de Souza VC, Corado A de L, Nascimento F, Silva G, et al. COVID-19 in Amazonas, Brazil, was driven by the persistence of endemic lineages and P.1 emergence. Nat Med. Nature Research; 2021;27:1230–8.

12. Covid-19: Bahia recomenda suspensão de viagens para 32 cidades do estado | VEJA.

13. Taxonomy History - Taxonomy - ICTV [Internet]. [cited 2021 Sep 30]. Available from: https://talk.ictvonline.org/taxonomy/p/taxonomy-history?taxnode_id=20185008

14. Hoover EA, Mullins JI. Feline leukemia virus infection and diseases. J. Am. Vet. Med. Assoc. 1991. p. 1287–97.

15. Powers JA, Chiu ES, Kraberger SJ, Roelke-Parker M, Lowery I, Erbeck K, et al. Feline Leukemia Virus (FeLV) Disease Outcomes in a Domestic Cat Breeding Colony: Relationship to Endogenous FeLV and Other Chronic Viral Infections. J Virol. American Society for Microbiology; 2018;92.

Tables

Table 1. Presence of SARS-CoV-2 RNA in tissues. The results are express as *Mean±SD* of CT values for N, E, and RdRP genes.

Tissues	CT Values of target genes		
	N [a]	E [b]	RdRP [c]
Spleen	23.39±0.16	27.50±0.57	33.72±0.58
Liver	22.46±0.21	22.11±0.36	26.04±0.09
Heart	26.34±0.18	25.43±0.48	28.14±0.26
Lungs	28.16±0.21	28.48±0.41	31.98±0.56
Trachea	16.04±0.1	15.16±0.06	16.98±0.23
Intestines	30.93±0.26	30.87±1,2	36.33±0.39
Kidneys	29.81±0.4	29.27±0.3	33.91±0.93

1. Nucleoprotein gene;
2. Envelope gene;
3. RNA-dependent RNA polymerase (RdRP) gene.

Figures

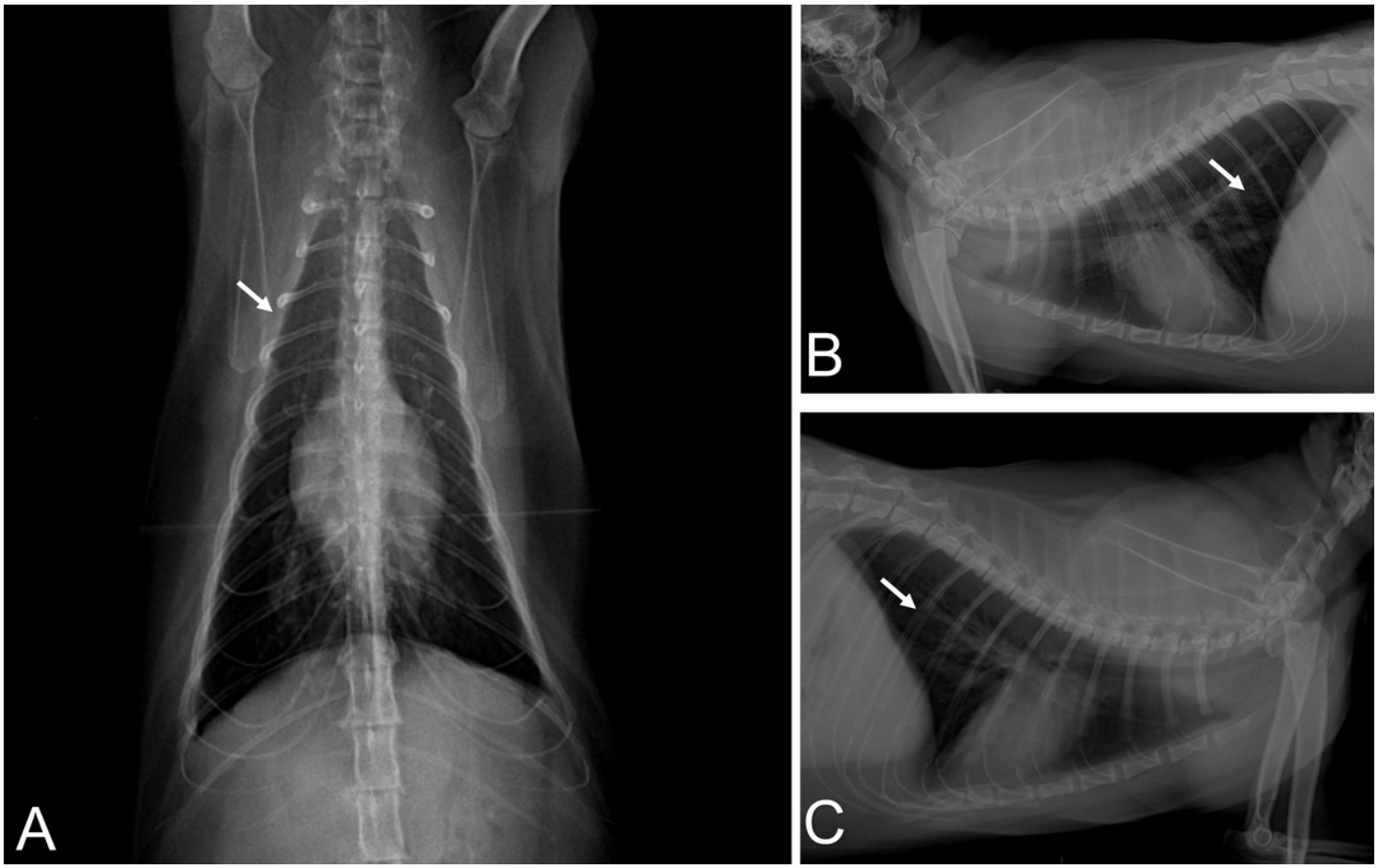

Figure 1

Radiographic views of ventrodorsal (A) lateral side (right and left, respectively) (B and C) showing increased radiopacity in the cranial and caudal lobes of both lungs accompanied by peribronchial infiltrate (white arrows) demonstrating incipient bronchitis.

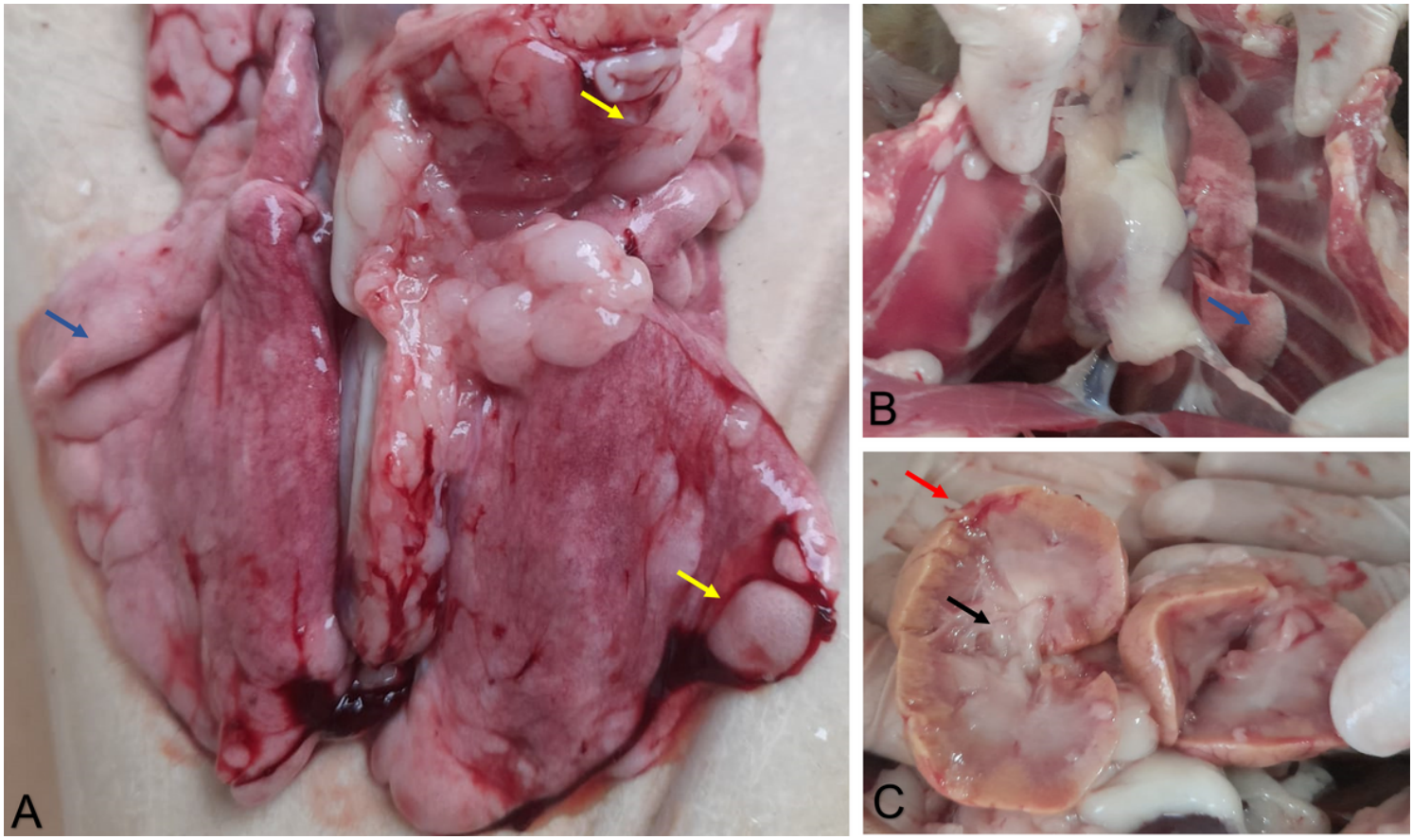

Figure 2

A and B: lungs showing atelectasis (blue arrows) and emphysematous areas (yellow arrows). C: kidneys showing cortical decrease (red arrow) and catarrhal-like secretion in the calyx and pelvis (black arrow).

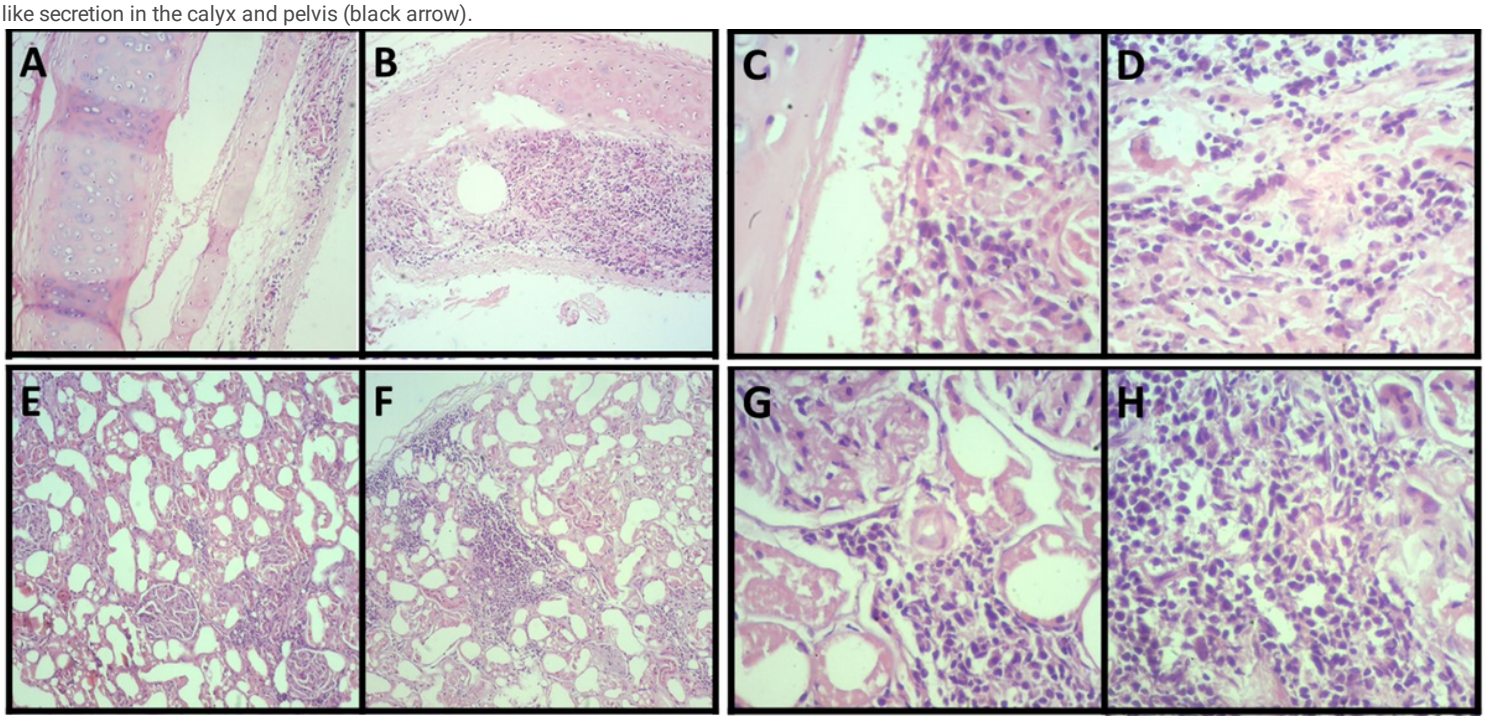

Figure 3

Moderate multifocal lymphoplasmacytic tracheitis. Photomicrography shows a piece of hyaline cartilage without alterations and artifactual distancing from tissue planes and moderate inflammatory infiltrate consisting predominantly of lymphocytes and plasma cells occupying the submucosa of the organ at 40x (A and B) and 400x (C and D) magnifications. Moderate lymphoplasmacytic interstitial nephritis. Photomicrograph shows the interstitial distribution of inflammation consisting predominantly of lymphocytes and plasma cells at 40x (E and F) and 400x (G and H) magnifications.

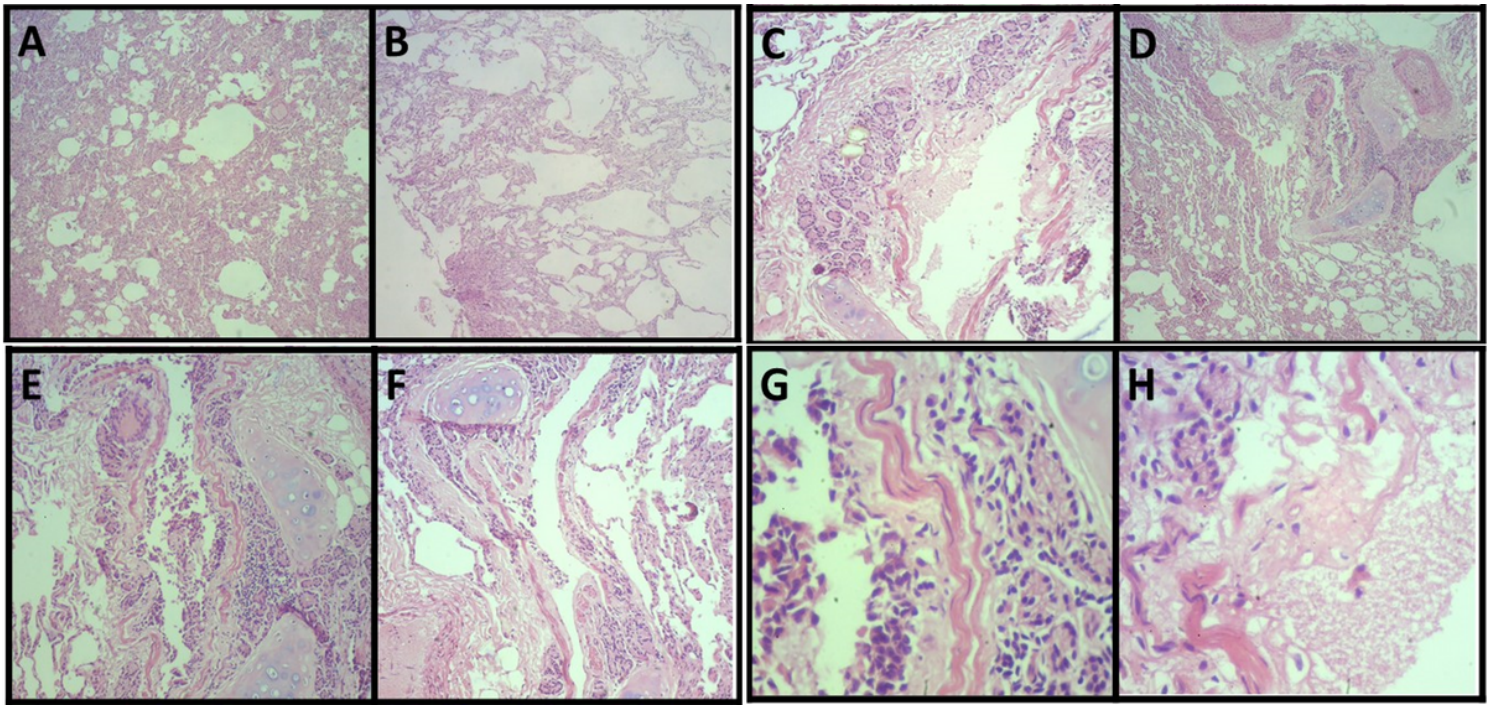

Figure 4

Lung parenchyma exhibits multifocal atelectasis at a magnification of 40x (A) and compensatory areas of emphysema at 40x magnification (B). Mild lymphoplasmacytic bronchitis. Photomicrography shows a sparse inflammatory infiltrate consisting predominantly of lymphocytes and plasma cells permeating the peribronchial mucous glands at 40x (A, B, C and D), 100x (E and F) and 400x (G) magnifications.

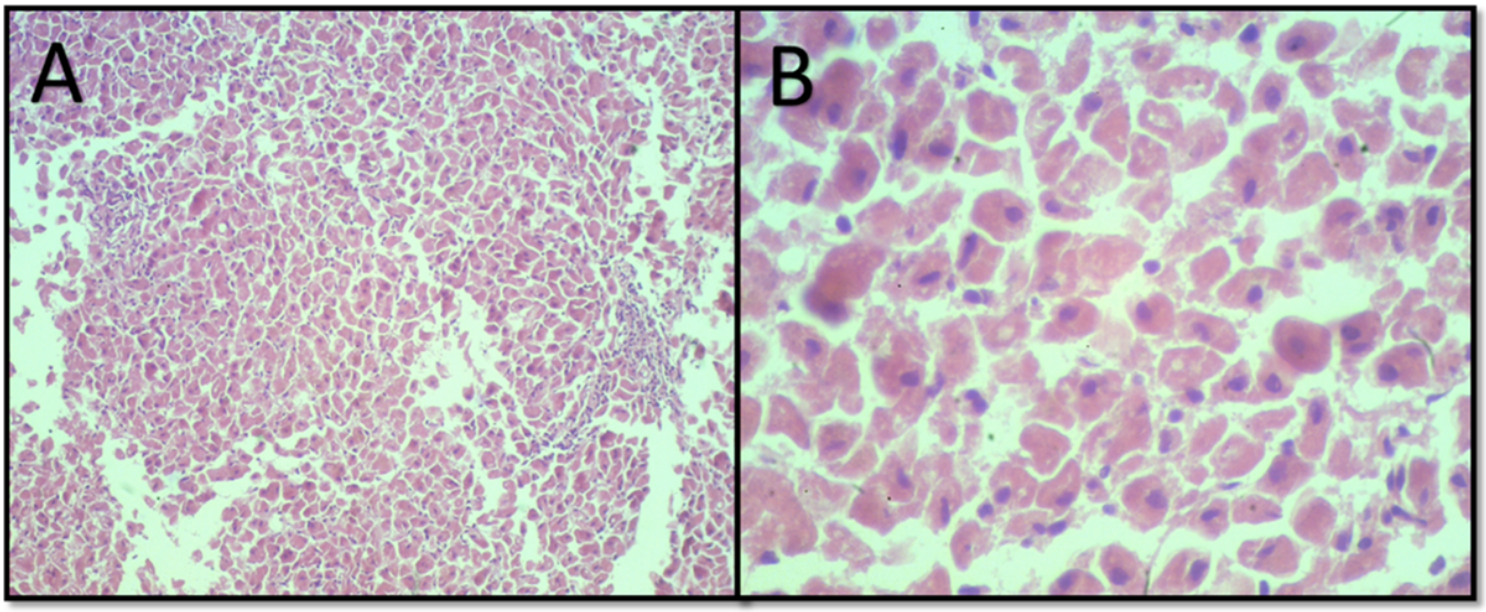

Figure 5

Mild lymphoplasmacytic periportal hepatitis. A sparse inflammatory infiltrate consisting predominantly of lymphocytes and plasma cells are seen at 100x magnification (A) and a mild vacuolar degeneration is seen at 400x magnification (B).

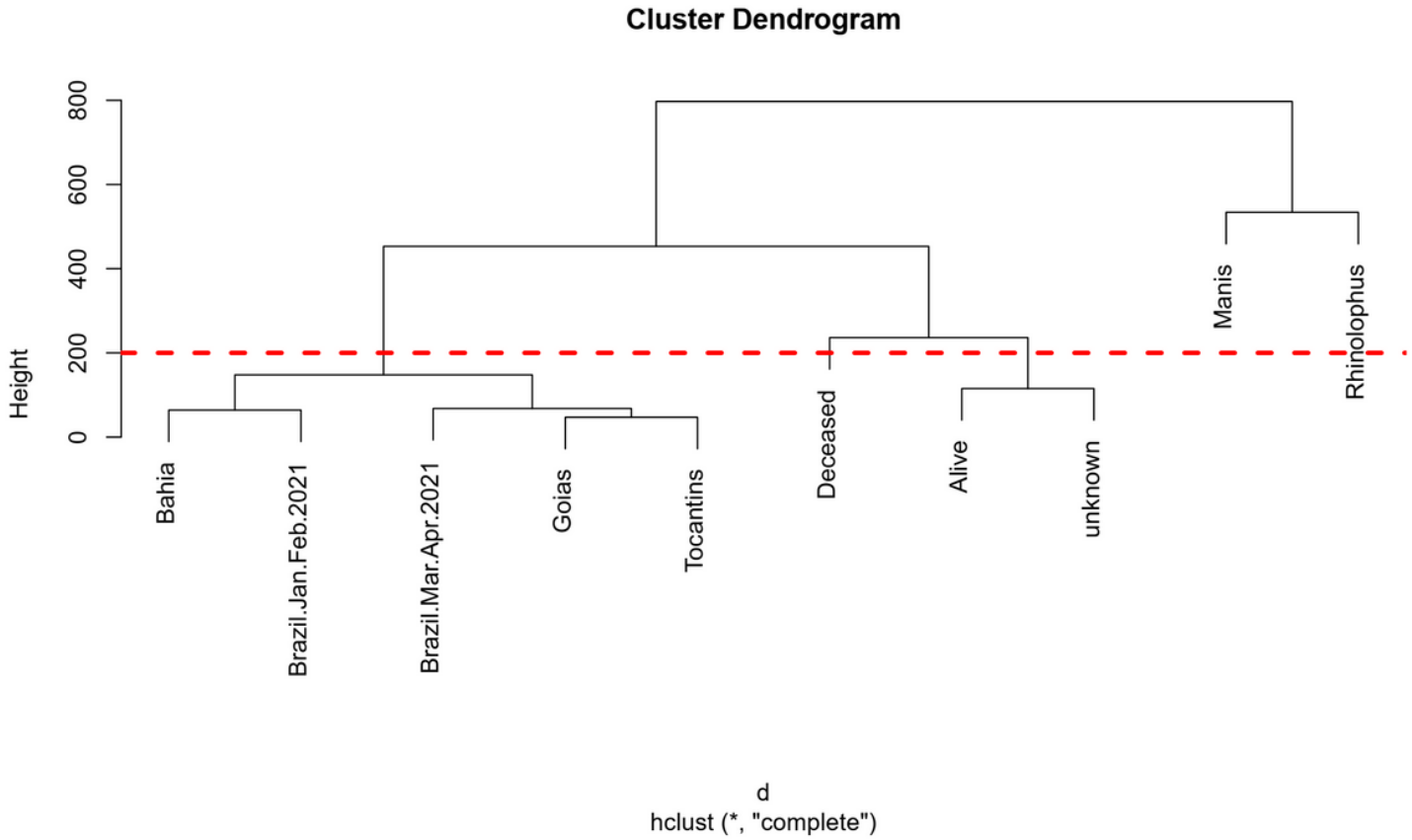

Figure 6

Unsupervised Hierarchical Clustering of mutation frequencies identified in FASTA sequences from several groups used for comparison.

Supplementary Files

This is a list of supplementary files associated with this preprint. Click to download.

- Suppdatasheet1.xls
- Supp.datasheet2.xls
- Supp.Fig.1.pdf
- Supp.Fig.2.pdf